A Characterization of Tight Sandstone

Effect of Clay Mineralogy on Pore-Framework

AlKharraa, Hamad Salman; Wolf, Karl Heinz A.A.; Kwak, Hyung T.; Deshenenkov, Ivan S.; AlDuhailan, Mohammed A.; Mahmoud, Mohamed A.; Arifi, Suliman A.; AlQahtani, Naif B.; AlQuraishi, Abdulrahman A.; Zitha, Pacelli L.J.

Citation (APA)
AlKharraa, H. S., Wolf, K. H. A. A., Kwak, H. T., Deshenenkov, I. S., AlDuhailan, M. A., Mahmoud, M. A., Arifi, S. A., AlQahtani, N. B., AlQuraishi, A. A., & Zitha, P. L. J. (2023). A Characterization of Tight Sandstone: Effect of Clay Mineralogy on Pore-Framework. In *Society of Petroleum Engineers - SPE Reservoir Characterisation and Simulation Conference and Exhibition 2023, RCSC 2023* (Society of Petroleum Engineers - SPE Reservoir Characterisation and Simulation Conference and Exhibition 2023, RCSC 2023). Society of Petroleum Engineers. https://doi.org/10.2118/212638-MS

Important note
To cite this publication, please use the final published version (if applicable).
Please check the document version above.

SPE-212638-MS

A Characterization of Tight Sandstone: Effect of Clay Mineralogy on Pore-Framework

Hamad Salman AlKharraa and Karl-Heinz A. A. Wolf, TU Delft; Hyung T. Kwak, Ivan S. Deshenenkov, and Mohammed A. AlDuhailan, Saudi Aramco; Mohamed A. Mahmoud and Suliman A. Arifi, KFUPM; Naif B. AlQahtani and Abdulrahman A. AlQuraishi, KACST; Pacelli L. J. Zitha, TU Delft

Abstract

Macro-, meso-, micro-pore systems combined with clay content are critical for fluid flow behavior in tight sandstone formations. This study investigates the impact of clay mineralogy on pore systems in tight rocks. Three outcrop samples were selected based on their comparative petrophysical parameters (Bandera, Kentucky, and Scioto). Our experiments carried out to study the impact of clay content on micro-pore systems in tight sandstone reservoirs involve the following techniques: Routine core analysis (RCA), to estimate the main petrophysical parameters such as porosity and permeability, X-ray diffraction (XRD), and scanning electron microscopy (SEM) to assess mineralogy and elemental composition, Mercury Injection Capillary Pressure (MICP), Nuclear Magnetic Resonance (NMR), and Micro-Computed Tomography (Micro-CT) to analyze pore size distributions. Clay structure results show the presence of booklets of kaolinite and platelets to filamentous shapes of illite. The Scioto sample exhibits a micro-pore system with an average pore body size of 12.6 ± 0.6 μm and an average pore throat size of 0.25 ± 0.19 μm. In Bandera and Kentucky samples illite shows pore-bridging clay filling with an average mineral size of around 0.25 ± 0.03 μm, which reduces the micro-pore throat system sizes. In addition, pore-filling kaolinite minerals with a diameter of 5.1 ± 0.21 μm, also reduce the micro-pore body sizes. This study qualifies and quantifies the relationship of clay content with primary petrophysical properties of three tight sandstones. The results help to advance procedures for planning oil recovery and CO_2 sequestration in tight sandstone reservoirs.

Introduction

Tight oil and gas reservoirs have to be developed to meet the growing energy demand (Sakhaee-Pour et al., 2014; Qu and Guo et al., 2020; Zeeshan et al., 2021) for a growing world population. Describing fluid flow at micro-and meso-scale in tight formations is challenging due to the complexity of the pore systems. Diagenesis is one of the main causes of the heterogeneity in pore systems of tight rocks. However, secondary mineral dissolution and recrystallization are additional elements of the burial history that complicate the spatial quantification of a pore-framework (Schmidt & Mcdonald, 1984; Lai et al., 2018).

Several studies show a comparable pore system complexity regarding the presence of clay minerals (Randolph et al., 1984; Soeder et al., 1987; Zhao et al., 2017). They represent significant mineral quantities in sedimentary rocks, such as sandstones. The minerals belong to the phyllosilicates, have a wide variety of physical and chemical properties, and are characterized in the optical properties molecular compositions of the mono-mineral flakes. (Coates et al., 1999; Rigby and Edler, 2002; Xiao et al., 2018) Clay minerals occupy the pores in three main modes: pore-filling, pore lining, and pore bridging (Neasham, 1977), where each mode impacts the basic petrophysical properties in a different manner. Illite minerals strongly reduce porosity and permeability of sandstone rocks (Moore and Reynolds, 1997). In addition, the presence of kaolinite booklets and illite pore bridging mineralization are responsible for lowering permeability and effective porosity in sandstone rocks (Schmitt et al., 2015).

To the best of our knowledge, the effect of clay minerals on micro-pore systems have rarely been discussed in the literature. Micro-pore systems are defined as consisting of pore-throats and pore-bodies having diameters less than 1 and 10 microns, respectively (Swanson, 1985; Keighin, 1997; Nelson, 2009). Because of the complexity of the pore system at different scales in tight sandstones, a full characterization of the micro-pores, with a combination of assessing methods is needed (Ren et al., 2019). We characterized the micro-pore systems in tight rocks by using image analysis with petrographical texture quantification on thin sections; SEM/Micro-CT/NMR imaging, and complementary MICP, and XRD analyses (Akin et al., 2003; Pan et al., 2015; Gao et al., 2016). Each technique provides independently unique spatial and mineralogical information and the insight into the distribution behavior within micro-pore system results (Dullien 1979; Wang et al., 2021; Wu et al., 2022).

XRD is used to determine the bulk mineral distribution with an emphasis on the clay mineral composition, and quantification of its structured grain part in the texture. Observing the micro-pores in tight rocks is impossible with this bulk analysis method (Coker et al., 1996; Liu et al., 2017). Tiny pores and distribution of clay minerals in micro-pore system have to be identified and qualified by using SEM (Jian, 2005; Yang et al., 2016), Micro-CT for quantification of pore body distributions (Tucker, 2001; Kwak et al., 2018; Meng et al., 2021), and especially in tight rocks, at higher resolution, in order to capture the small pore bodies (Klaver et al., 2016). Additionally, MICP is used to determine pore throat size distribution of the open pore framework (Katz and Thompson, 1986; Liao et al., 2012; Xiao et al., 2017). However, narrow throat sizes may impede flow rate because of the reduced rock permeability and resulting rising capillary pressure. Drainage and imbibition processes are more challenging to perform and need careful attention (Darcy, 1856; Cao et al., 2016). Hence, high mercury injection pressure was suggested to be used to estimate micro-pore throat sizes distributions in tight sandstones (Kilmer et al., 1987; Zou et al., 2012).

NMR is an alternative to quantify bulk micro-pore systems and system variations in tight rocks (Chen and Balcom, 2006). Based on NMR measurements, pore volumes of micro-, meso-, and macro-pore systems in sandstones can be determined by analyzing T_2 cutoff values (Mitchell et al., 2014; Kwak et al., 2017). The threshold or T_2 cutoff is the intersection value between 1) the cumulative curves of NMR T_2 fully brine saturated, and 2) the NMR T_2 after drainage process. Values below this intersection represent the trapped fluid within small pores immobile to flow. Values above T_2 cutoff, correspond to hydrogen molecules, which are free to move (Timur, 1969; Sen et al., 1990). In sandstones, the T_2 cutoff value is experimentally determined to be approximately 33 msec. However, it may vary, since the T_2 relaxation is affected by pore geometry (Coates et al., 1999). The T_2 relaxation time from a big pore is longer and progressively shorter as the pore size decreases from large to medium to small (Hinedi et al., 1997).

The study is structured as follows. The first step is to describe the experimental methods and workflow as used in this study. The results of these experiments are then explained and discussed accordingly. Finally, a discussion and conclusions are followed by recommendations.

Experiments

Bandera, Kentucky, and Scioto sandstone outcrops were received from Kocurek Industries Caldwell, TX in a cleaned and dried condition. The samples were analyzed on their porosity by using NMR, MICP, and Micro-CT results. A step-by-step procedure for each experiment conducted in this study is shown in Figure 1.

Figure 1—The workflow diagram of the current study.

NMR T_2 measurements were performed on sandstone cores fully saturated with brine and after drainage processes to estimate the fluid volume in pore systems. In the NMR measurements 3% KCL brine was used to saturate samples for the T_2 measurements at Sw=1. A centrifuge with a rotational speed of 4,000 was then used to reach the immovable fluid volume. In the MICP tests, mercury was used to produce capillary pressure curves, from which the throat size distributions were determined.

An Auto Pore V 9600 was performed on three cylindrical plugs of rock samples 0.5 × 0.5-inch diameter to obtain the pore-throat distribution. The maximum injection pressure performed on the three samples reaches 60,000 psi, which enables access to the micro-pore throat system.

Porosity was determined by using a Vinci™ helium porosimeter and the application of Boyle's law. The absolute permeability was measured by using a Core-Lab™ Gas Permeameter. A TESCAN instrument model MIRA3 equipped with EDX detector was used to create SEM images. Mineral determination was done by using X-ray diffraction analysis. Rock chips of the three sandstones prepared as thin disks of around 5 mm diameter and a volume of ca. 10 mm³, were prepared in advance. A Rigaku ULTIMA IV powder X-Ray diffractometer ran with a Cukα radiation source at 40 kV and 40 mA with 2θ interval, covering the range from 3° to 100° with a step size of 0.02° increment of 8 minutes.

The Micro-CT tests were performed on cylindrical plugs with a diameter of 4.3 mm and a length of 4.1 mm. The resulting stacked images, i.e. 3D tomograms, were further analyzed on the pore body size distributions. The test was carried out on a Zeiss Xradia Versa-620 CT-scanner using an X-ray source with 100 KV/7 W energy settings and, providing a total of 5001 images. The voxel size for three sandstone samples is 5 μm.

A 2 MHz Oxford Instruments GeoSpec 2−75 equipped with Green Imaging Technologies Systems v6.1 software. The NMR test was conducted on cylindrical plugs of rock samples with a 1.5-inch diameter and 1.5-inch length at 25 °C. The T_2 relaxation times for all the samples were determined by the Carr-Purcell-Meiboom-Gill pulse sequence (Carr and Purcell, 1954). NMR T_2 spectrums were measured using 110 μs echo spacing and 150 signal to noise ratio.

Results and Discussion

Porosity and Permeability

Porosities and permeabilities are summarized in Table 1. Scioto and Kentucky samples were found to have nearly similar porosity permeability 17.5 vol. % and permeability of 1.21 mD for Scioto, and 15vol.

% porosity and 0.98 mD permeability for Kentucky. Bandera has a higher porosity of 25 vol.% and considerable higher permeability of 24 mD.

Table 1—Porosities and permeabilities of three sandstone samples.

Sandstone name	Porosity (%)	Permeability (mD)
Bandera	25± 0.10	24± 0.20
Kentucky	15± 0.10	0.98± 0.20
Scioto	17.5± 0.10	1.21± 0.20

Mineralogy and Pore-system analysis

The XRD and SEM results show that for the three sandstones that quartz (SiO_2) is the dominant mineral, associated by small amounts of feldspar and clay minerals (Figure 2). Bandera sample has the highest percentage of clay, 14 wt%. The Kentucky and Scioto samples have a total clay content ranging from 3 to 4 wt%. Furthermore, XRD analyses indicates that illite is the most abundant clay mineral in all samples, with approximately 6.4 wt% in the Bandera sample, 3.6 wt% in the Kentucky sample, and 2.2 wt% in the Scioto sample. The results also show that Bandera has the highest kaolinite clay content of 4.5 wt%, followed by Scioto with almost 1.0 wt %.
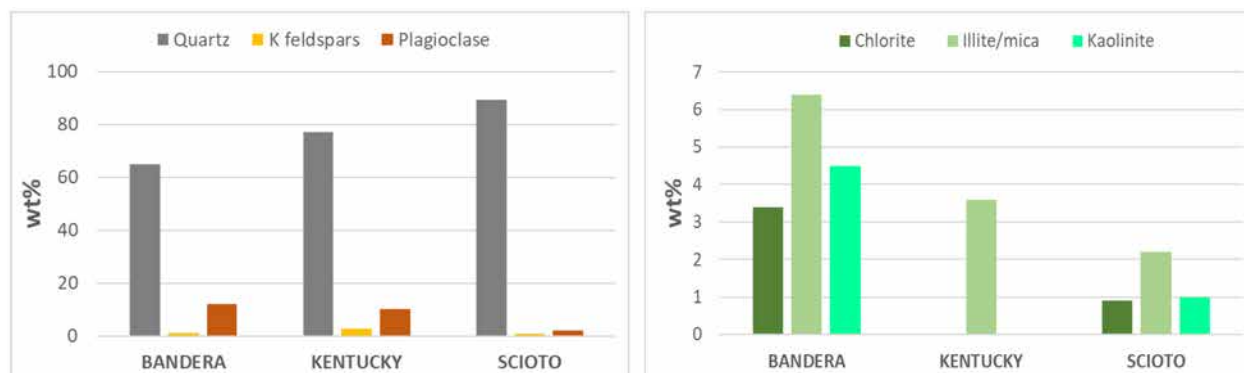

Figure 2—Bulk minerals determined by XRD of Bandera, Kentucky, and Scioto sandstone samples. (left) Quartz and feldspar minerals content, and (right) clay minerals content.

The distribution of these minerals in the micro-pore system visualized and quantified using the SEM microphotographs (Figure 3), show that the pore-filling kaolinite is predominant in Bandera sample, whereas filamentous illite form pore bridging structures in Bandera and Kentucky sandstones. These results are in good agreement with the XRD mineral analysis results.
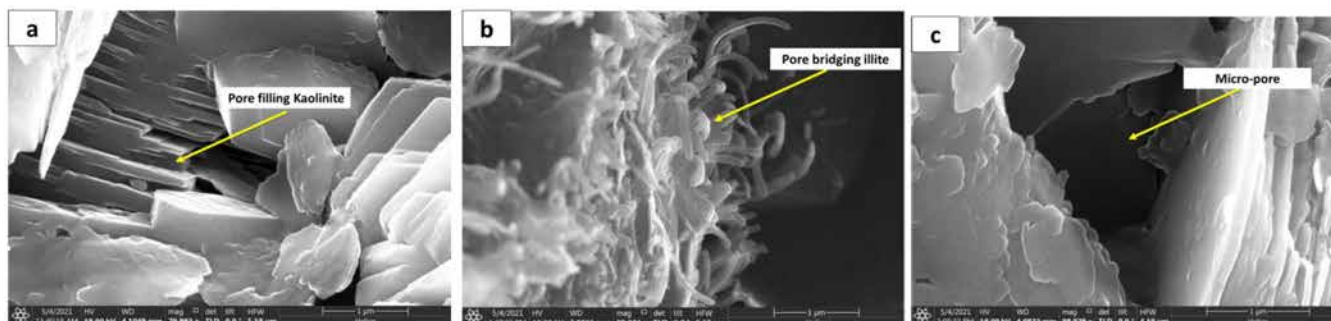

Figure 3—SEM images represent (a) pore filling with kaolinite booklets, (b) pore bridging with illite filaments

NMR T_2 measurements were performed at Sw=1, saturated with brine, and after drainage conditions in order to estimate the fluid volume in the pore systems (Figure 4). The NMR T_2 distribution of the brine-saturated samples shows a dominant single peak and represents the pore size distribution of the sandstone samples. It is clearly visible that the Bandera sample contains a larger pore size distribution compared to the other samples, having the longest T_2 peak at 40 ms, followed by the Scioto sample with T_2 peak at 35 ms, and the smallest pore size distribution is the Kentucky sample, which shows the shortest relaxation peak of 28 ms. After evacuation and removal of all brine, the non-wetting phase (air), generates no NMR signal since it contains no hydrogen molecules (Karimi and Kazemi, 2015). Subsequently, the immovable fluid can be determined by subtracting the drainage NMR T_2 spectrum from fully saturated brine NMR T_2 spectrum (Figure 4). Fluid distribution in macro-, meso-, and micro-regimes can then be calculated for sandstone samples.
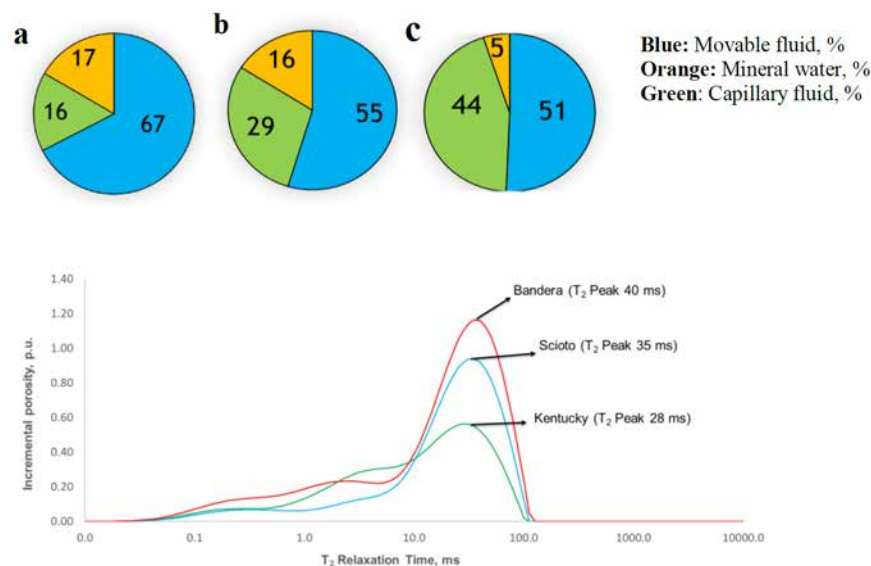

Figure 4—NMR T_2 results for three sandstone samples (a) Bandera, (b) Kentucky, (c) Scioto.

Figure 5-a shows the micro-pore throat distributions for the three sandstone samples from the MICP measurements. We confirm that, on one hand, the micro-pore throat system of Kentucky and Bandera samples is low, representing respectively 6 and 8 vol. %. However, the Scioto, has a much higher micro-pore throat system of nearly 29 vol. %. We also confirm that the decrease in micro-pore throat system, in Bandera and Kentucky samples is due to illite bridging that blocks the tiny pores. It was also confirmed by using the NMR T_2 measurements, where irreducible fluid in Kentucky and Bandera samples is also low 45 and 33%, respectively when compared to Scioto sandstone of almost 50% (Figure 4). Micro-CT results show that Kentucky has the highest micro-pore body system of 29.6%. On the contrary, Bandera and Scioto show low micro-pore body system due to the high kaolinite content of 4.5 and 1.0 wt% (Figure 5-b).
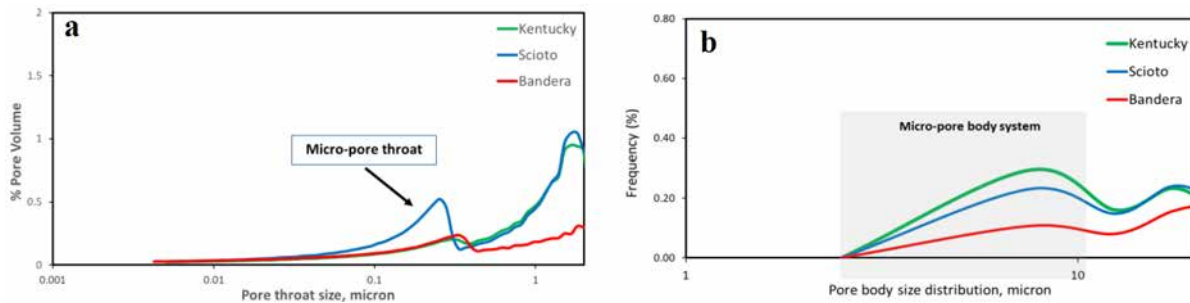
Figure 5—Micro-pore size distribution results (a) micro-pore-throat distribution, (b) micro-pore body distribution.

Impact of clay minerals on micro-pore system. It is confirmed that micro-pore system can be identified using the workflow as proposed in Figure 1. MICP results show that illite clay minerals reduce the micro-pore throat distribution in Bandera and Kentucky samples. This observation is in line with the NMR T_2 results, where the immovable volume shows lower values. NMR T_2 results also illustrate the immovable fluid is the largest among the tested sample. Therefore, this shows that illite blocks the micro-pore systems and reduces the immovable fluid volume accordingly. In addition, Micro-CT results confirm that kaolinite reduces the micro-pore body sizes in Bandera and Scioto samples. These results align with SEM images where kaolinite fills the tiny pores (Figure 3-b).

Conclusion

Several imaging and spatial measurement techniques were applied on the Bandera, Kentucky, and Scioto sandstone to investigate their micro-pore systems and their impact on the petrophysical properties of the sandstone. The techniques included the routine core analysis to estimate the main petrophysical parameters of porosity and permeability; X-ray diffraction (XRD), and scanning electron microscopy (SEM) to determine the mineralogical and recognize the presence of clay minerals within the pore system; Mercury intrusion capillary pressure (MICP) for pore throat size distributions analysis, nuclear magnetic resonance (NMR) and Micro-Computed Tomography (Micro-CT) to analyze pore size distributions. Based on this study, following conclusions can be made:

- A workflow to characterize the impact of clay minerals on micro-pore throats and bodies in tight rocks was developed
- SEM results identify illite clay mineral blocking the micro-pore throats in Bandera and Kentucky sandstone samples. Kaolinite clay fills the small pores in Scioto and Bandera.
- Pore size and mineralogical results confirmed that presence of illite reduces the micro-pore throat system size. Pore filling kaolinite lowers the micro-pore bodies size in sandstone samples.
- Presence of kaolinite and illite reduce the micro-pore system size significantly.

- NMR T_2 measurements and MICP results show that micro-pore system contribution of Bandera and Kentucky samples is relatively small compared to Scioto samples due to presence of clay minerals.
- The accessibility of the micro-pore system in the Scioto sample is better than other samples due to the lack of pore-bridging illite.
- We recommend to include more tight sandstone samples in this study.

Acknowledgment

References

Akin, S. and Kovscek, A. R. 2003. Computed Tomography in Petroleum Engineering Research. *Geological Society*, London, Special Publications **215** (1): 23–38.

Carr, H., and Purcell, E., 1954. Effects of Diffusion on Free Precession in Nuclear Magnetic Resonance Experiments. *Physical Review* **94**(3):630–638.

Cao, Z., Liu, G., Zhan, H., Li, C., You, Y., Yang, C. and Jiang, H., 2016. Pore structure characterization of Chang-7 tight sandstone using MICP combined with N2GA techniques and its geological control factors', *Scientific Reports*, **6**(1), 1–13.

Chen, Q., and Balcom, B. J., 2006. A Single-Shot Method for Capillary Pressure Curve Measurement Using Centrifuge and Quantitative Magnetic Resonance Imaging. Presented at SPE/DOE Symposium.

Coates, G.R., Xiao, L., and Manfred, G.P. 1999. NMR Logging Principles and Applications: Halliburton Energy Services Publication H02308.

Coker D., Torquato S., Dunsmuir J., 1996. Morphology and physical properties of Fontainebleau sandstone via a tomographic analysis. *Journal of Geophysical Research* **101**: 17,497–517.

Darcy, H., 1856. *Les Fontaines Publiques de la Ville de Dijon*. Paris: Victor Dalamont.

D. Kwak, S. Han, J. Han, J. Wang, J. Lee, Y. Lee, 2018. An experimental study on the pore characteristics alteration of carbonate during waterflooding, *J. Pet. Sci. Eng.*

Dullien, F. A. L. 1979. Porous Media-Fluid Transport and Pore Structure. Academic Press, New York.

Gao, H., Li, H., 2016. Pore structure characterization, permeability evaluation and enhanced gas recovery techniques of tight gas sandstones. *J. Nat. Gas Sci. Eng.* 2016, **28**, 536–547.

Hinedi, Z.R., Chang, A.C., Anderson, M.A., Borchardt, D.B., 1997. Quantification of microporosity by nuclear magnetic resonance relaxation of water imbibed in porous media. *Water Resour. Res.* **33**, 2697–2704.

Jian H., 2005. Water flooding microscopic seepage mechanism research based on three-dimension network model. *Chinese Journal of Theoretical and Applied Mechanics*. **37**. 783–787.

Karimi, S., and Kazemi, H., 2015. Capillary Pressure Measurement using Reservoir Fluids in a Middle Bakken Core. Presented at the SPE Western Regional Conference held in Garden Grove, California, 27-30 April. SPE 174065-MS.

Katz, A. J., and Thompson, A. H., 1986. Quantitative prediction of permeability in porous rock. *American Physical Society, Physical Reviews B*, **34**,8179–8181.

Kaixuan Qu and Shaobin Guo, 2020. *Investigation of the Pore Structure of Tight Sandstone Based on Multifractal Analysis from NMR Measurement: A Case from the Lower Permian Taiyuan Formation in the Southern North China Basin*. Washington, DC: US Department of the Interior, US Geological Survey.

Keighin, C.W. 1997. Physical Properties of Clastic Reservoir Rocks in the Uinta, Wind River, and Anadarko Basins, As Determined by Mercury-injection Porosimetry. *USGS Bull*. **2146**: 73–83.

Kilmer, N.H., N. R. Morrow, and J. K. Pitman, 1987. Pressure sensitivity of low permeability sandstones: *Journal of Petroleum Science and Engineering*, v. **1**, p. 65–81.

Klaver J., Desbois G., Littke R., Urai J.L., 2016. BIB-SEM pore characterization of mature and post mature Posidonia Shale samples from the Hils area, Germany. *Int J Coal Geol*.

Kwak, H.T., Wang, J. and AlSofi, A.M. 2017. Close Monitoring of Gel-based Conformance Control by NMR Techniques, SPE paper 183719, presented at the SPE Middle East Oil and Gas Show and Conference, Manama, Kingdom of Bahrain, March 6-9, 2017.

Lai, J., Wang, G., Cao, J., Xiao, C., Wang, S., Pang, X., Dai, Q., He, Z., Fan, X., Yang, L. 2018. Investigation of pore structure and petrophysical property in tight sandstones.

Liao J., Tang H., Zhu X., Ren M., Sun Z., Lin D., 2012. Water sensitivity experiment and damage mechanism of sandstone reservoirs with ultra-low permeability: a case study of the eighth oil layer in the Yanchang Formation of Xifeng oilfield, Ordos Basin.

Liu K., Ostadhassan M., 2017. Quantification of the microstructures of Bakken shale reservoirs using multi-fractal and lacunarity analysis. *J Nat Gas Sci Eng*. 2017;**39**:62–71.

Mitchell, J., Fordham, E.J., 2014. Contributed Review: nuclear magnetic resonance core analysis at 0.3 T. *Rev. Sci. Instrum*. **85**, 111502. https://doi.org/10.1063/1.4902093.

Moore, D. M. & Reynolds, R. C., 1997. X-Ray Diffraction and the Identification and Analysis of Clay Minerals, 2nd ed. xviii + 378 pp. Oxford, New York: Oxford University Press.

Neasham J.W. 1977. The morphology of dispersed clay in sandstone reservoirs and its effect on sandstone shaliness, pore space and fluid flow properties. *In Proceedings of the 52nd Annual Technical Conference Effect of pore geometry on Gassmann fluid substitution.*

Nelson, P.H., Pore-throat sizes in sandstones, tight sandstones, and shales. *AAPG Bulletin*, 2009. **93**(3): p. 329–340.

Pan, S., Zou, C., Yang, Z., Dong, D., Wang, Y.; Wang, S., Wu, S.; Huang, J., Liu, Q., Wang, D. 2015. Methods for shale gas play assessment: A comparison between Silurian Longmaxi shale and Mississippian Barnett shale. *J. Earth Sci.* 2015, **26**, 285–294.

Randolph, P. L., D. J. Soeder, and P. Chowdiah, 1984. Porosity and permeability of tight sands: 1984 Society of Petroleum Engineers/U.S.Department of Energy/Gas Research Institute Unconventional Gas Recovery Symposium, Pittsburgh, Pennsylvania, SPE Paper 12836, 10 p.

Ren X., Li A., Fu S., Tian W., 2019. Influence of micro-pore structure in tight sandstone reservoir on the seepage and water-drive producing mechanism—a case study from Chang 6 reservoir in Huaqing area of Ordos basin. *Energy Sci Eng*. 2019;**00**:1–13.

Rigby, S.P. and Edler, K.J. 2002. The Influence of Mercury Contact Angle, Surface Tension, and Retraction Mechanism on the Interpretation of Mercury Porosimetry Data, *J Colloid Interface Sci*. **250** (1): 175–190. doi: 10.1006/jcis.2002.8286.

Sakhaee-Pour, A.; Bryant, S.L. Effect of pore structure on the producibility of tight-gas sandstones. *AAPG Bull*. 2014, **98**, 663–694.

Schmidt, V. and Mcdonald, D. A. 1984. Secondary Reservoir Porosity in the Course of Sandstone Diagenesis. *AAPG Continuing Education Course Note Series*, 12.

Schmitt, M., Fernandes, C.P., Wolf, F.G., da Cunha, J.A.B.Neto, Rahner, C.P., dos Santos, V.S.S., 2015. Characterization of Brazilian tight gas sandstones relating permeability and Angstrom-to micron-scale pore structures. *J. Nat. Gas Sci. Eng*. **27**, 785–807.

Sen, P.N., Straley, C., Kenyon, W.E., and Whittingham, M.S., 1990, Surface-to-volume ratio, charge density, nuclear magnetic relaxation and permeability in clay-bearing sandstones: *Geophysics*, v.**55**, no 1,p.61–69.

Soeder, D. J., and P. L. Randolph, 1987. Porosity, permeability, and pore structure of the tight Mesaverde Sandstone, Piceance Basin, Colorado: *Society of Petroleum Engineers Formation Evaluation*, v. **2**, no. 2, p. 129–136.

Swanson, B.F., 1985. Microporosity in reservoir rocks: its measurement and influence on electrical resistivity. J.SPWLA2198369.

Timur, A., 1969. Producible porosity and permeability of sandstone investigated through nuclear magnetic resonance principles. *Log. Anal*. **10**, 9.

Tucker M., 2001. *Sedimentary petrology—revised*. Blackwell Science Inc, Oxford.

Wang, W., La, W., Fan, T., Xu, X., Liu, Y., and Lv, Q. 2021. A Comparative Study on Microscopic Characteristics of Volcanic Reservoirs in the Carboniferous Kalagang and Haerjiawu Formations in the Santanghu Basin, China. *Front. Earth Sci*. **9**, 728.

Wu K, Chen D, Zhang W, Yang H, Wu H, Cheng X, Qu Y and He M, 2022. Movable Fluid Distribution Characteristics and Microscopic Mechanism of Tight Reservoir in Yanchang Formation, Ordos Basin.

Xiao, D., Jiang, S., Thul, D., Huang, W., Lu, Z., and Lu, S. 2017. Combining Rate-Controlled Porosimetry and NMR to Probe Full-Range Pore Throat Structures and Their Evolution Features in Tight Sands: A Case Study in the Songliao Basin, China. *Mar. Pet. Geology*.

Xiao, D., Jiang, S., Thul, D.; Lu, S., Zhang, L., Li, B. 2018. Impacts of clay on pore structure, storage and percolation of tight sandstones from the Songliao Basin, China: Implications for genetic classification of tight sandstone reservoirs. *Fuel* 2018, **211**, 390–404.

Yang R., He S., Yi J., Hu Q., 2016. *Nano-scale pore structure and fractal dimension of organic-rich Wufeng-Longmaxi shale from Jiaoshiba area, Sichuan Basin: Investigations using FE-SEM, gas adsorption and helium pycnometry.*

Zeeshan T., Muhammad S., K., Mohamed M., Mobeen M., Abdulazeez A., and Xianmin Z., 2021. *Dicationic Surfactants as an Additive in Fracturing Fluids to Mitigate Clay Swelling: A Petrophysical and Rock Mechanical Assessment ACS Omega* 2021 **6** (24).

Zhao, P., Wang, Z., Sun, Z., Cai, J., Wang, L., 2017. Investigation on the pore structure and multifractal characteristics of tight oil reservoirs using NMR measurements: Permian Lucaogou Formation in Jimusaer Sag, Junggar Basin. *Mar. Pet. Geol*.

Zou, C., Zhu, R., Wu, S., Yang, Z., Tao, S., Yuan, X., Hou, L., Yang, H., Xu, C., Li, D., 2012. Types, characteristics, genesis and prospects of conventional and unconventional hydrocarbon accumulations: taking tight oil and tight gas in China as an instance. *Acta Pet*.